Percutaneous Steerable Robotic Tool Delivery Platform and Metal Microelectromechanical Systems Device for Tissue Manipulation and Approximation: Closure of Patent Foramen Ovale in an Animal Model

Nikolay V. Vasilyev, Andrew H. Gosline, Evan Butler, Nora Lang, Patrick J. Codd, Haruo Yamauchi, Eric N. Feins, Chris R. Folk, Adam L. Cohen, Richard Chen, David Zurakowski, Pedro J. del Nido and Pierre E. Dupont

Circ Cardiovasc Interv. 2013;6:468-475; originally published online July 30, 2013;
doi: 10.1161/CIRCINTERVENTIONS.112.000324
Circulation: Cardiovascular Interventions is published by the American Heart Association, 7272 Greenville Avenue, Dallas, TX 75231

Print ISSN: 1941-7640. Online ISSN: 1941-7632

Percutaneous Steerable Robotic Tool Delivery Platform and Metal Microelectromechanical Systems Device for Tissue Manipulation and Approximation

Closure of Patent Foramen Ovale in an Animal Model

Nikolay V. Vasilyev, MD; Andrew H. Gosline, PhD; Evan Butler, MS; Nora Lang, MD; Patrick J. Codd, MD; Haruo Yamauchi, MD, PhD; Eric N. Feins, MD; Chris R. Folk, PhD; Adam L. Cohen, BS; Richard Chen, MS; David Zurakowski, PhD; Pedro J. del Nido, MD; Pierre E. Dupont, PhD

Background—Beating-heart image-guided intracardiac interventions have been evolving rapidly. To extend the domain of catheter-based and transcardiac interventions into reconstructive surgery, a new robotic tool delivery platform and a tissue approximation device have been developed. Initial results using these tools to perform patent foramen ovale closure are described.

Methods and Results—A robotic tool delivery platform comprising superelastic metal tubes provides the capability of delivering and manipulating tools and devices inside the beating heart. A new device technology is also presented that uses a metal-based microelectromechanical systems–manufacturing process to produce fully assembled and fully functional millimeter-scale tools. As a demonstration of both technologies, patent foramen ovale creation and closure was performed in a swine model. In the first group of animals (n=10), a preliminary study was performed. The procedural technique was validated with a transcardiac hand-held delivery platform and epicardial echocardiography, video-assisted cardioscopy, and fluoroscopy. In the second group (n=9), the procedure was performed percutaneously using the robotic tool delivery platform under epicardial echocardiography and fluoroscopy imaging. All patent foramen ovales were completely closed in the first group. In the second group, the patent foramen ovale was not successfully created in 1 animal, and the defects were completely closed in 6 of the 8 remaining animals.

Conclusions—In contrast to existing robotic catheter technologies, the robotic tool delivery platform uses a combination of stiffness and active steerability along its length to provide the positioning accuracy and force-application capability necessary for tissue manipulation. In combination with a microelectromechanical systems tool technology, it can enable reconstructive procedures inside the beating heart. **(*Circ Cardiovasc Interv*. 2013;6:468-475.)**

Key Words: catheters ■ heart septal defects ■ robotics ■ surgery

Catheter-based therapies for structural heart disease have advanced significantly in recent years. The availability of novel imaging technologies and the development of new devices have enabled the introduction of a variety of percutaneous and transcardiac procedures. These include aortic valve replacement,[1] mitral valve repair and replacement,[2] and closure of septal defects.[3,4] Most of the current catheter-based techniques, however, are fundamentally focused on device deployment rather than patient-specific reconstruction of the intracardiac tissue. This is principally because of shortcomings of current catheter delivery systems, including limitations on the ability to apply and control forces sufficient for tissue manipulation, as well as limitations on the ability to position the tip with respect to moving cardiac tissue.

Although robotically assisted delivery systems can potentially overcome these problems, current robotic systems have been used predominantly to aid catheter navigation toward a target and to ensure that contact forces are uniform but small, so as to create desired lesions, while avoiding perforation. While these technologies are useful for atrial fibrillation ablation procedures, as well as complex coronary artery and peripheral interventions,[5–8] they are not designed to enable complex reconstructive procedures, which require precise tissue grasping and approximation.

This article describes a robotic tool delivery platform (TDP) designed to enable beating-heart reconstructive procedures. The robotic TDP was evaluated in the context of patent foramen ovale (PFO) closure using a metal microelectromechanical

Received December 26, 2012; accepted June 17, 2013.

From the Department of Cardiac Surgery (N.V.V., A.H.G., E.B., N.L., P.J.C., H.Y., E.N.F., P.J.d.N., P.E.D.) and Departments of Anesthesia and Surgery, Boston Children's Hospital and Harvard Medical School, Boston, MA (D.Z.); and Microfabrica Inc, Van Nuys, CA (C.R.F., A.L.C., R.C.).

Guest Editor for this article was Jeffrey A. Brinker, MD.

Correspondence to Nikolay V. Vasilyev, MD, Department of Cardiac Surgery, Boston Children's Hospital, Harvard Medical School, 300 Longwood Avenue, Boston, MA 02115. E-mail nikolay.vasilyev@childrens.harvard.edu

Circ Cardiovasc Interv **is available at http://circinterventions.ahajournals.org** **DOI: 10.1161/CIRCINTERVENTIONS.112.000324**

WHAT IS KNOWN

- Currently available robotic catheters are not designed to perform tissue reconstructive procedures inside the beating heart.
- Most of the currently available devices for catheter-based closure of patent foramen ovale are large frame-based septal occluders and devices that are inserted inside the patent foramen ovale channel.
- The availability of fully functional millimeter-scale tools that can be used to perform image-guided beating-heart intracardiac reconstructive procedures and can be deployed at the tips of catheters is currently limited.

WHAT THE STUDY ADDS

- To address these limitations, this article introduces a catheter-like robotic tool delivery platform composed of curved metal tubes that is substantially stiffer than standard catheters and is also steerable along its entire length.
- A tissue approximation device is also described that mimics surgical closure of patent foramen ovale and provides minimal exposure of foreign material on the left side of the heart with the ability to adjust the force to avoid excessive tissue compression.

systems (MEMS) tissue approximation device that mimics the patient-specific approximation achieved in open-heart surgery.

Methods

Robotic TDP

The TDP is a new type of robotic catheter that is composed of a set of concentrically combined precurved superelastic metal tubes (Figure 1).[9] The curvatures of the individual tubes interact elastically to produce the overall curvature of the device. By using coordinated rotations and translations of the tubes at their proximal ends using a computer-controlled motorized drive system (Figure 1A), the extended length, shape, and tip position can be precisely controlled.[9] Although these devices, known as concentric tube robots, are substantially stiffer than standard catheters, they can provide the capability to be safely deployed inside the heart because the shape along their entire length can be actively controlled. Similar to a catheter, they possess a lumen along their entire length enabling introduction and exchange of tools and devices.

The set of tubes comprising the robot is designed on a procedure-specific basis to provide the family of shapes needed: (1) to navigate through the vasculature to the desired chamber of the heart and (2) to provide the distal tip motions required to manipulate tools and tissue to perform the desired intervention. Although the robot extends in a telescopic fashion, a unique feature is that the shape (ie, curvature and length) of each telescoping section can be independently controlled. In particular, each section can be designed to possess either a specific fixed curvature or a curvature that can be actively varied between straight and maximally curved configurations. When a section is retracted, it conforms to the shape of the proximal section. When it is extended, it relaxes elastically to its resting curvature. According to the requirements of the procedure, the number of sections and the variability of curvature for each section can be selected to enable navigation to the surgical site as well as to provide 6 degrees of freedom for positioning the robot tip.

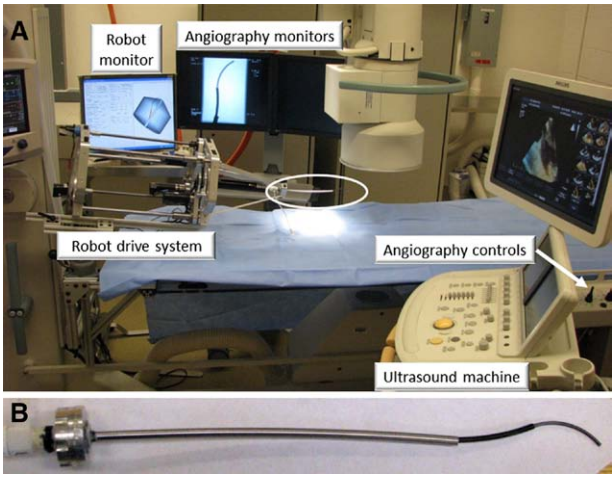

Figure 1. The equipment layout in the operating room. **A**, Motorized drive system and robot tube set (circled) comprising tool delivery platform mounted on operating room table. Monitors behind table display computed robot shape and fluoroscopic image. **B**, Assembled 4-tube robot used for transjugular patent foramen ovale closure.

For PFO closure, the motor drive system (Figure 1A) is attached to the operating table and is positioned, as shown in Figure 2A, to align the tube set for introduction into the right internal jugular vein. The robot tube set designed for this procedure is composed of 4 tubes arranged in 3 telescopically extending sections (Figure 1B). The proximal section consists of a single tube of constant curvature that is extended from the point of percutaneous entry in the jugular vein to the superior vena cava–right atrium (RA) junction. Once positioned, this section of the robot is locked for the remainder of the procedure. The distal 2 telescoping sections are then actively controlled to perform the tissue approximation for PFO closure. Figure 2B depicts several configurations of the robot to illustrate the workspace (set of tip configurations) that can be reached with this tube set.

Robot Navigation

Robot motion can be controlled using 2 different modes of operation. The first mode consists of controlling tip position and orientation using a 6 degree-of-freedom joystick. In this mode, a computer controller converts translation and rotation commands from the joystick into coordinated motions of the tube set that produce the desired robot tip position and orientation inside the heart. This mode of control is particularly effective during parts of a procedure when specific relative motions of the robot tip are desired (eg, when manipulating tissue). The second control mode enables independent control of the degrees of freedom of each tube via a graphical user interface (Figure 1A) and keyboard commands. This mode is especially effective for controlling the overall shape of the robot to accomplish safe navigation inside the

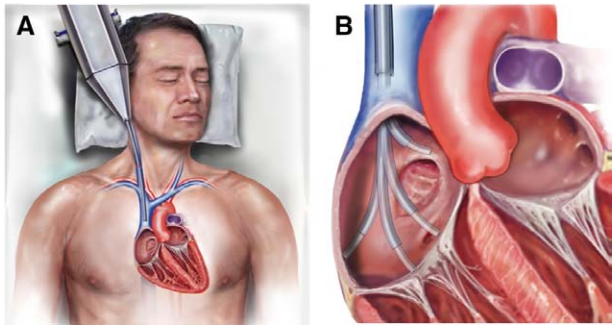

Figure 2. A, Placement of tool delivery platform with respect to patient for transjugular access. **B**, Four possible configurations of the tool delivery platform of Figure 1B within the right atrium.

heart. In both modes, a graphical interface displays, in real time, the current shape of the robot. This display can be used in combination with various imaging modalities, such as 2D and 3D ultrasound and fluoroscopy (Figure 1A), to navigate the robot inside the heart.

Robot Tip Stiffness

The capability of applying forces to manipulate tissue inside the heart depends on the stiffness of the robot at its tip. Catheter-based deployment devices are stiffest when loaded along their longitudinal axis and most flexible in bending and twisting. Stiffness of the TDP was measured experimentally for the 2 configurations shown in Figure 3. These tests were conducted on the bench top at room temperature with the robot rigidly supported at its base, but unsupported along its length. The 215-mm long configuration of Figure 3A is representative of the procedural configurations that are used to puncture the septum secundum (longitudinal stiffness) and to stretch the septum secundum over the septum primum (lateral stiffness). To achieve tissue penetration, a stylet consisting of a sharpened stainless steel wire is inserted through the robot lumen. The stylet contributes to robot bending stiffness but not to torsional stiffness and also produces a small reduction in robot curvature. Results are reported with and without the stylet.

The configuration of Figure 3B is the most extended (flexible) configuration used during PFO closure (245-mm long) and corresponds to the configuration in which the robot is extended into the left atrium (LA). For each of the tested configurations, known forces were applied to the robot tip in the longitudinal (axial) and lateral coordinate directions, F_a and F_l, respectively. The lateral coordinate direction is selected to generate maximum bending and twisting in the tube set so as to maximize flexibility. Forces were applied using a scale (Scout Pro 200 g, ±0.01 g, Ohaus Corp, Pine Brook, NJ) mounted on a vertical linear stage (Model 443, Newport Corp, Irvine, CA) with displacement measured using a digital height gage (Tormach, ±0.04 mm). Stiffness was determined by measuring robot tip displacement associated with each applied load and correcting the measured displacement for load-based scale deflection.

Two-way ANOVA was applied to assess the effect of load and use of stylet on axial and lateral stiffness for each of the 2 TDP configurations, with the interaction F test (load-by-stylet) used to compare slopes to determine whether the stylet increases robot stiffness. Two-tailed $P<0.05$ was considered statistically significant. Statistical analysis was performed using the Mixed GLM Procedure in SPSS version 19.0 (SPSS Inc/IBM, Chicago, IL).

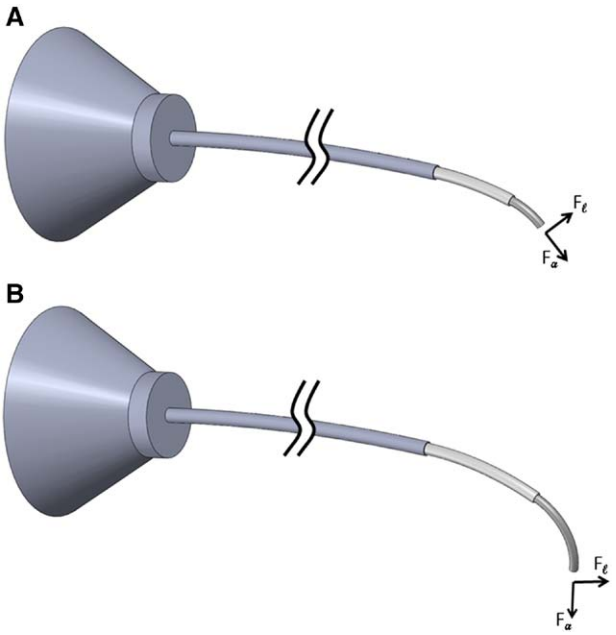

Figure 3. A, Tool delivery platform (TDP) configuration (215-mm length) used for stiffness testing that corresponds to axial puncture and lateral stretching of the septum secundum. **B**, TDP configuration (245-mm length) used during patent foramen ovale closure corresponding to tip extension into the left atrium. F_a and F_l indicate axial and lateral applied loads.

Tissue Approximation Device

A tissue approximation device was designed with the clinical goal of replicating surgical PFO closure by suture. The design of the device is described in detail by Butler et al[10] and briefly summarized here. These devices were fabricated using an innovative metal MEMS process (Microfabrica Inc, Van Nuys, CA) in which many devices are simultaneously manufactured fully assembled.[11] In contrast to existing catheter-delivered occlusion devices,[3] the approximation device shown in Figure 4A is designed to introduce a minimal amount of foreign material into the LA, to provide the capability of adjusting the degree of tissue approximation (ie, force applied) on a patient-specific basis and to be removable during the procedure if device deployment proves unsatisfactory. The device consists of a ratcheting mechanism connecting 2 sets of folding wings. When folded, the device can be passed through a 1.6-mm diameter lumen. Device operation (Figure 4B–4E) is controlled using a wire and surrounding tube.

Figure 5 illustrates the steps by which 2 tissue layers can be approximated. In the first step, the robot is positioned at the desired spot on the first tissue layer, the septum secundum. Then, a stylet, extended from the robot tip, is used to puncture the first tissue layer. The robot is then extended through the puncture and the septum secundum is then stretched as needed to achieve the desired overlap with the second tissue layer, the septum primum. This maneuver ensures sealing of the RA entry into the PFO channel. The stylet is subsequently extended through the second layer followed by the robot tip. The stylet is then removed and the approximation device is advanced through

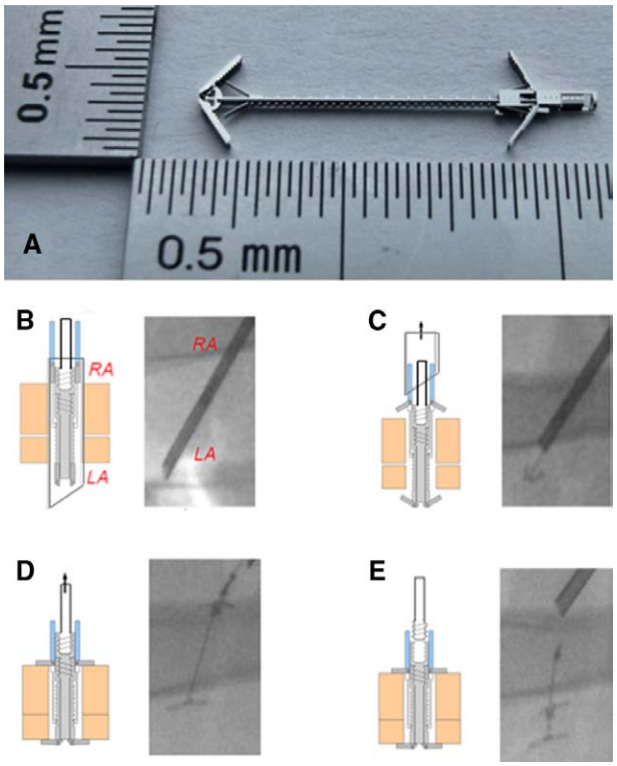

Figure 4. A, Photograph of the metal microelectromechanical systems tissue approximation device. **B** through **E**, Schematic depicting deployment sequence of tissue approximation device with corresponding fluoroscopic image during manual instrument patent foramen ovale closure. **B**, Penetration through both layers of the septum. **C**, Deployment of distal wings. **D**, Deployment of proximal wings and ratcheting to achieve approximation. **E**, Release of device. LA indicates left atrium; and RA, right atrium.

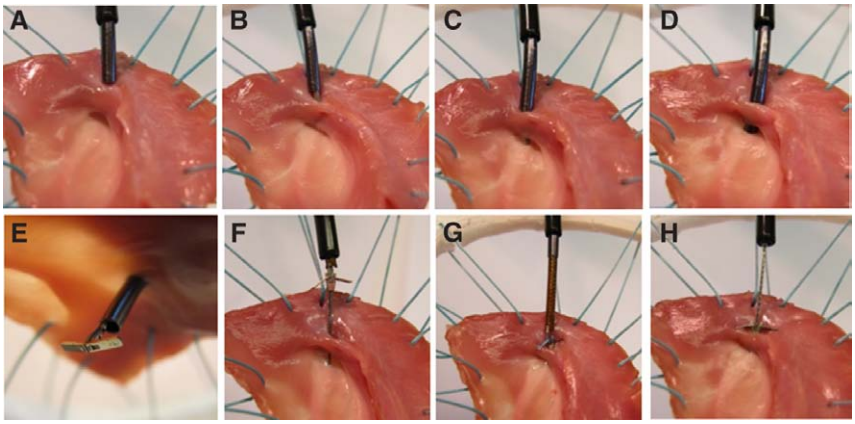

Figure 5. Procedural steps of robotic PFO closure illustrated on an ex vivo porcine septum. **A**, Positioning TDP on ridge above the PFO channel. **B**, Stylet puncture of the septum secundum. **C**, Stretching of the septum secundum over the septum primum. **D**, Stylet penetration of the septum primum followed by dilation and puncture using distal robot tube into LA. **E**, Deployment of distal wings in LA. **F**, Retraction of TDP into right atrium and deployment of proximal wings. **G**, Adjusting ratchet to achieve desired approximation of the PFO channel. **H**, Release of device. LA indicates left atrium; PFO, patent foramen ovale; and TDP, tool delivery platform.

the robot lumen until the distal wings of the device are opened inside the LA as shown in Figure 5E. Leaf springs cause the wings to extend and, as the robot is retracted, the wings extend fully against the distal tissue layer, the LA side of the septum. The robot tip is now retracted further such that the proximal wings are exposed and spring open on the RA side of the septum (Figure 5F). Relative translation of the deployment tube and wire causes the pairs of extended wings to pull the tissue layers together by the desired amount, resulting in complete sealing of the PFO channel. The device is released by rotating the deployment wire clockwise, as shown in Figure 5H. If deployment is deemed unsuccessful, the device can be removed by rotating the deployment wire counterclockwise causing the distal wings to fold outward so that it can be withdrawn through the tissue layers.

For system integration purposes as well as for procedure development, the TDP and the tissue approximation device were initially tested ex vivo on a bench-top simulator and with in vivo swine model experiments without PFO creation.[12]

Animal Experiments

The experimental protocol was approved by the Boston Children's Hospital Institutional Animal Care and Use Committee. All animals received humane care in accordance with the 1996 Guide for the Care and Use of Laboratory Animals recommended by the US National Institute of Health. The 60- to 70-kg Yorkshire pigs were anesthetized by intramuscular injection of tiletamine/zolazepam (7 mg/kg) and xylazine (4 mg/kg), intubated with a cuffed endotracheal tube and ventilated with a volume control ventilator (Hallowell EMC Model 2000, Hallowell EMC, Pittsfield, MA). Anesthesia was maintained with 2% to 3% isoflurane.

The animals were divided into 2 groups. In the first group (n=10), a preliminary study was performed. A PFO animal model was established, and the PFO closure procedure was validated using a transcardiac hand-held delivery system for the MEMS approximation device. A midline sternotomy was performed, and a 4-0 Prolene purse-string suture was placed on the RA appendage for instruments and device insertion. After initial assessment of the anatomy by epicardial echocardiography using the X7-2 matrix transducer on an IE33 system (Philips Healthcare, Andover, MA), heparin was administered at 150 U/kg IV, and a tunnel-like PFO was created under video-assisted cardioscopy and epicardial echocardiography guidance. A cardioport system, previously described by Vasilyev et al[13] was used for cardioscopy. Briefly, the cardioport has 2 compartments: 1 for imaging and 1 for instrument insertion and exchange. The inner imaging compartment of the cardioport has an exchangeable transparent plastic bulb at the end. It houses a standard 5-mm endoscope for imaging. When the cardioport is introduced into a cardiac chamber and the blood between the tip of the bulb and the tissue target is displaced, direct visualization of the tissue is possible. The outer working channel is 3 mm in diameter and is used for instrument access. PFO creation was confirmed by 2D and 3D epicardial echocardiography. Then, for PFO closure, the hand-held deployment system was advanced toward the atrial septum. Once the septum was penetrated, fluoroscopy (XRE corporation angiography station, Littleton, MA) was used for device deployment and ratcheting.

In the second group of animals (n=9), the percutaneous concentric tube robotic TDP was tested. A right side neck cutdown approach was performed and the right internal jugular vein was indentified. The TDP was introduced via a transjugular approach via 16-Fr introducer sheath (Cook Medical Inc, Bloomington, IN) and advanced toward the RA under ultrasound guidance. Once the delivery system was positioned on the septum using robotic controls, the PFO closure was performed using the MEMS tissue approximation device, using the technique described above.

The procedures were performed by a single operator, who was a trained cardiovascular surgeon with prior experience in development of image-guided cardiac procedures (N.V.V.) and an assistant. The equipment layout in the operating room is shown on Figure 1A. The operator controlled the angiography station and the ultrasound system. An assistant, positioned on the opposite side of the table, operated the concentric tube robotic controls taking commands from the operator. Completion of PFO closure was confirmed by 2D and 3D echocardiography and color Doppler imaging. The acquisitions were performed simultaneously with manual single-breath positive-pressure ventilation, to better assess the left-to-right shunting through the PFO channel. Finally, the animals were euthanized, the heart was excised, and the efficacy of the procedure was determined by means of direct inspection. The inner surface of the superior vena cava–RA junction, the RA walls, and the tricuspid valve were inspected for potential damage from the delivery system. The position of the MEMS approximation device and the completeness of the PFO closure were determined.

Results

Robot Tip Stiffness

Robot displacement/load data for axial stiffness is shown in Figure 6A, where the maximum stiffness achieved without stylet was 112.7 g/mm for the 215-mm configuration and 34.2 g/mm for the 245-mm configuration. Results based on ANOVA revealed that for the 215-mm configuration, stylet insertion had no significant effect on displacement (P=0.15), whereas displacement was significantly reduced with stylet insertion for the 245-mm configuration (P<0.001). Robot displacement/load results for lateral stiffness are depicted in Figure 6B, where the maximum stiffness achieved without stylet was 54.3 g/mm for the 215-mm configuration and 14.8 g/mm for the 245-mm configuration. Stylet insertion increased displacement slightly for the 215-mm configuration (P=0.003), although this effect was small and of little interest scientifically; however, for the 245-mm configuration, ANOVA confirmed a highly significant reduction in lateral displacement when the stylet was inserted (P<0.001).

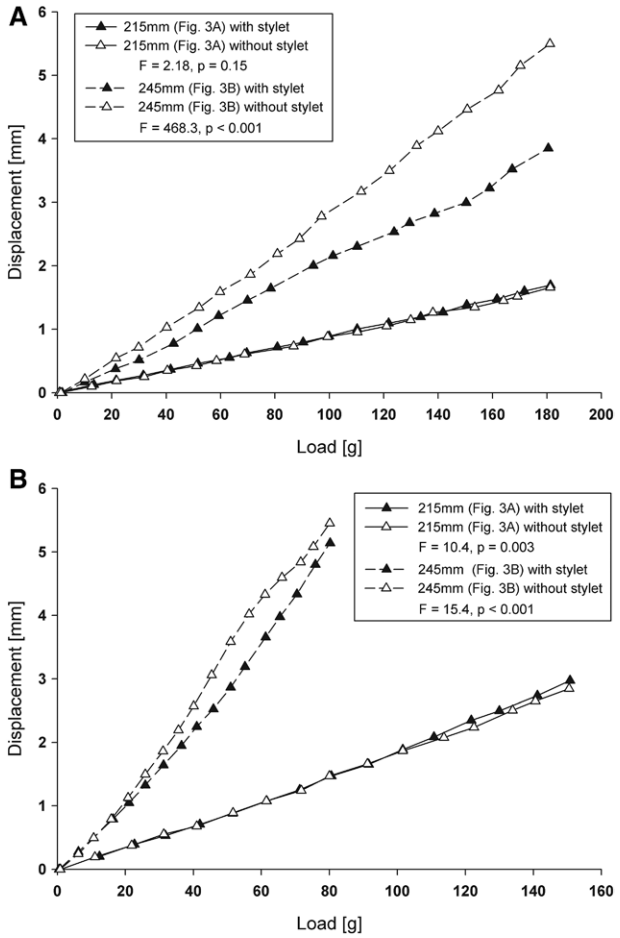

Figure 6. Measured displacement vs load of tool delivery platform with and without stylet. **A**, Axial loading direction. **B**, Lateral loading direction.

PFO Creation

In Group 1, a PFO was created under combined video-assisted cardioscopy and 2D and 3D epicardial echocardiography guidance in the first 3 animals. The cardioport was introduced into the RA via a purse-string suture and advanced toward the atrial septum. The area between the septum primum and the septum secundum was identified, and a guide wire was advanced between the septa under cardioscopic guidance. This created an initial PFO channel communication. The cardioport was then removed, and a series of precurved dilators, up to 20 Fr, were introduced to enlarge the PFO channel. In all subsequent animals, because we became more confident with echocardiography image guidance, PFO creation was completed solely under echocardiography guidance using a modified right-angle surgical clamp. The clamp was positioned on the septum between the septum primum and the septum secundum under 2D and 3D echocardiography guidance. Then, the clamp was advanced and the channel was enlarged by spreading the branches of the clamp. This technique was used for 6 animals. Separation between the septum primum and the septum secundum was confirmed by echocardiography. One animal was found to have a naturally occurring PFO.

In the second group, all but one of the PFOs were successfully created using the modified right-angle clamp technique as described above. In 1 case, after multiple attempts, it was not feasible to separate the septa, which led to creation of a 3×5-mm atrial septal defect. One animal had a naturally occurring PFO.

PFO Closure

In Group 1, all the PFOs were successfully closed. One device per animal was used in 9 cases, and in 1 case, 2 devices were deployed side by side. In the first 2 animals, cardioscopy was used to navigate the deployment system toward the spot of the septum secundum puncture. The straight hand-held delivery system, composed of a sharpened 14-Ga needle, was introduced into the instrument channel of the cardioport and advanced toward the target under cardioscopy guidance. The septum secundum was punctured, and its ridge was stretched over to overlap the septum primum. Then, the septum primum was punctured, and the delivery system was advanced toward the LA. The cardioport was then withdrawn from the RA. Under fluoroscopy guidance, the distal wings of the MEMS approximation device were opened, and the entire system was moved back until the distal wings touched the LA side of the atrial septum (Figure 4B–4E). Contact was clearly visible on the fluoroscopy image as a flattening of the wings. Then, the delivery system was further withdrawn into the RA, resulting in the opening of the proximal wings. Finally, the device was ratcheted to bring the 2 sets of wings, and the septum secundum and the septum primum, respectively, together, sealing the PFO channel. The device was then disconnected from the delivery system. In all the subsequent cases, the delivery system was positioned on the septum, and the described maneuvers were performed solely under 2D and 3D echocardiography guidance and fluoroscopy. No residual shunts were detected, and no anatomic structures were compromised in any of the cases.

In Group 2, the concentric tube robotic system enabled percutaneous performance of the maneuvers that were established with the hand-held delivery system. In all cases, a stylet was inserted through the robot lumen for use in puncturing the septum primum and septum secundum. After stylet puncture, the distal robot tube was extended through the tissue layer. Once the robotic delivery system reached the LA, the stylet was removed through the proximal end of the robot's lumen and the device was manually loaded in its place. The device was then deployed manually, whereas the robotic tube set operated under motorized control. The steps of device deployment were identical to those established during the experiments in Group 1. In the animal in which an atrial septal defect was created, it was determined that there was insufficient septum primum in which to deploy the device, and the procedure was abandoned. The PFO was completely sealed in 6 out of the 8 remaining cases using 1 device per animal, which was confirmed by echocardiography (Figure 7) and postmortem examination (Figure 8). A residual shunt was detected in 1 case, and it was observed that TDP positioning too far superior to the edge of the septum secundum prevented complete tissue overlap of the septum primum. In another case, a robot tube set with incorrect curvature was used, resulting in an inability to reach the desired location for penetration of the septum primum, leading to improper device placement. In all of the cases, no adverse events occurred and no surrounding anatomic structures were compromised.

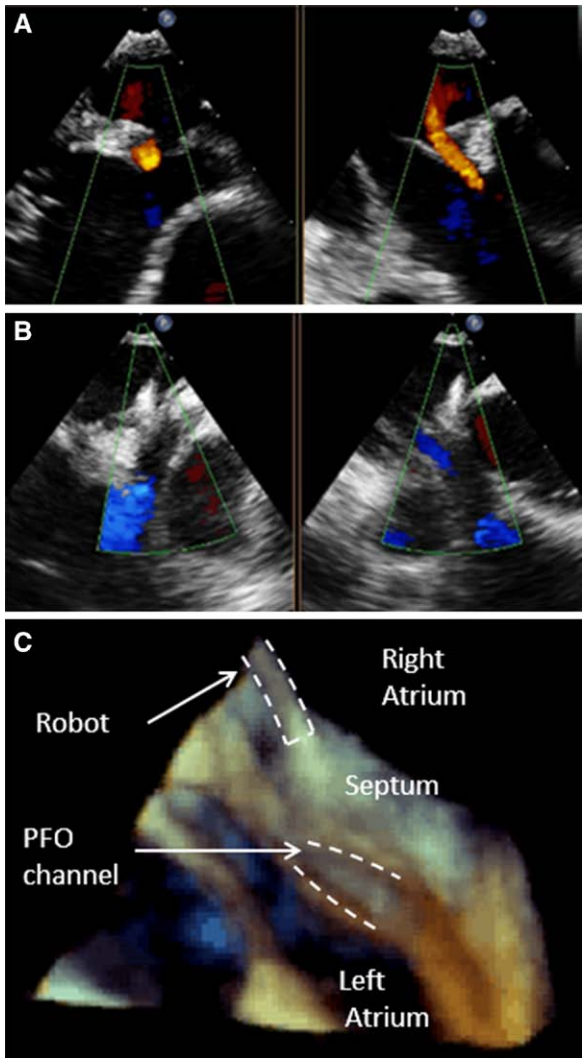

Figure 7. Epicardial echocardiography during robotic procedure. **A**, Confirmation of pre-existing PFO shunt via forced ventilation and biplane 2D color Doppler. **B**, Confirmation of closed PFO shunt after device deployment using forced ventilation and biplane 2D color Doppler. **C**, Real-time 3D echocardiography showing robot positioned on septal ridge above PFO channel. PFO indicates patent foramen ovale.

Discussion

We describe a novel robotic TDP designed to enable beating-heart reconstructive procedures. These robots are designed on a procedure-specific basis as sets of precurved tubes whose curvatures and lengths are algorithmically optimized to enable navigation to the desired locations within the heart and to provide the necessary degrees of freedom for tool and device operation. The TDP enables precise control of robot shape and tip position via independent control of each telescoping section in longitudinal increments of 1 mm and rotational (lateral) increments of 1 degree. These motion increments are procedure-dependent and potentially can be reduced further to allow even greater precision.

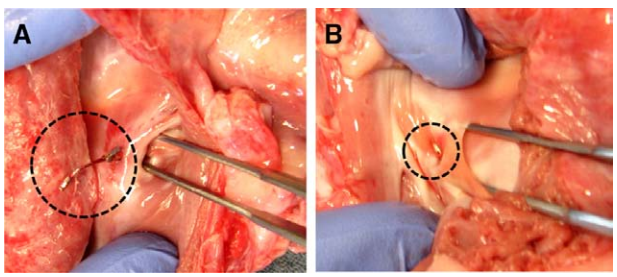

Figure 8. Postmortem confirmation of the device placement; the microelectromechanical systems device is depicted inside the dashed circles. **A**, Right atrial view. **B**, Left atrial view.

The position of the robot with respect to the intracardiac structures was visualized using combined real-time 3D echocardiography and fluoroscopy, which ensures safe navigation throughout the procedure. Unlike standard catheter-based systems, the robot does not require bracing against a vessel or cardiac chamber wall to flex toward a desired direction. Importantly, once the robot is positioned at the target location, the drive system immobilizes the TDP in the desired shape and location until additional motion commands are given. This is a key design feature of the TDP system, which ensures the operator of predictable and safe motion control. In the described experiments, it was possible to reach the target locations within the RA, while avoiding contact with the atrial free wall along the length of the robot extending from the superior vena cava.

Because the robot is composed of metal tubes, it can be designed to be substantially stiffer than a standard catheter and is, therefore, capable of applying larger forces in all tip directions as may be needed to manipulate tissues during reconstructive procedures. For the robot tube set used in these procedures, measured tip stiffness on the bench top with the length of the robot unsupported was 34.2 to 112.7 g/mm in the axial direction and 14.8 to 54.3 g/mm in the most compliant lateral direction, depending on tube extension and curvature. The capability to design steerable and yet stiff delivery devices provides the potential to develop new procedures and to create novel device designs.

Several robotic catheter navigation systems have been introduced with the goal of providing precise catheter navigation.[5–7] Similar to the robot described here, these systems enable catheter tip control from a remote station. The CorPath 200 system (Corindus Vascular Robotics, Natick, MA) uses standard guide wires and catheters. The Sensei X robotic navigation system, designed for electrophysiology interventions, and the Magellan system, a platform for peripheral vascular interventions, were introduced by Hansen Medical (Mountain View, CA). The Hansen systems use an actuated sheath steered by controlling tendon tension in a manner similar to manually steerable catheters. The Niobe magnetic navigation system (Stereotaxis, St. Louis, MO) and Magnetecs system (Catheter Guidance Control and Imaging, CGCI, Magnetecs, Los Angeles, CA) incorporate magnet-tipped catheters that move on the basis of forces and torques generated by external permanent magnets and electromagnets respectively. Although tip stiffness data for the Hansen system are unavailable, forces reported for magnetically powered catheters vary between 5 g at a 70-mm length and 27 g at a 30-mm length.[7] Because the magnetic field strength of the Stereotaxis system is less than that of the Magnetec system, it can be anticipated that its maximum forces are also less.[6]

In contrast, the high stiffness of the TDP proposed here enables the operator to produce substantial forces against

tissue, whereas the ability to control the robot's shape along its entire length facilitates safe operation. For the robot TDP lengths of 215 mm and 245 mm (without stylet) in the tested configurations (Figure 3A and 3B) producing the maximum catheter force of 27 g, reported by Gang et al,[7] would require axial tip deflections of 0.24 and 0.79 mm, respectively. In the lateral direction, this force would require tip deflections of 0.50 and 1.82 mm, respectively.

It will be important in future applications to monitor and control tissue contact forces at the tip. Catheter tip force sensors[8] could be easily integrated with the proposed system. Furthermore, motorized actuation of the system can enable automated computer-based control of contact force as well as stiffness.[14]

The TDPs positioning and force-application capabilities were demonstrated here by performing a percutaneous procedure in a completely novel way with the goal of recapturing the advantages of the surgical approach without the risks and side effects of cardiopulmonary bypass and open surgery. Our long-term objective is to develop a platform technology for reconstructive cardiac procedures that are currently performed through open surgery.

Tissue Approximation Device

The robotic TDP was evaluated in the context of PFO closure using a novel metal MEMS closure device that mimics the patient-specific approximation achieved in open surgery. The advantages of this device include (1) minimal exposure of foreign material on the left side of the heart, thereby promoting rapid endothelialization and (2) the ability to adjust the force applied between the approximated layers during deployment to ensure complete elimination of flow, while also avoiding excessive tissue compression that could lead to tissue erosion.

In contrast, most of the existing technologies used for PFO closure are large frame-based septal occluders, and devices that are inserted inside the PFO channel, which rely on elastic relaxation to block the channel.[3] Although recent clinical trials provide some evidence of a potential benefit to device-based PFO closure in adults with cryptogenic stroke,[4] there are disadvantages to any large foreign structure that stretches the atrial septum and is exposed to systemic circulation. Complications may include cardiac perforation or air embolization during implantation, device embolization, early and late thrombosis, atrial fibrillation, and tissue erosion. Furthermore, implantation of such devices may complicate future transseptal access to the LA.[15]

In summary, the robotic and tool technologies presented here represent promising initial efforts to provide instrumentation for beating-heart interventions that can enable the types of tissue manipulation that currently remain within the domain of open surgery. PFO closure was demonstrated here as an example in which a robotic platform could be used to stretch one tissue layer over another and in which a device could allow the clinician to tailor the approximation of tissue layers to the specific anatomy of the patient. Other applications may include percutaneous valve repair or replacement, arrhythmia ablation, closure of paravalvular leaks, and left atrial appendage occlusion, among other procedures via subclavian or transapical access. Further chronic animal studies will be required before implementation of this technique in clinical practice. Both the TDP delivery platform and the MEMS tissue approximation device would require additional testing that is necessary for regulatory clearance and approval.

Potential System and Study Limitations

The TDP described in this study has some potential limitations. The tube set comprising the robot was designed for transjugular access to the RA. Alternative access sites for procedures in other chambers of the heart would require the design of new tube sets. This is a 1-time event, however, because once the appropriate tube sets are known, they can be used for all similar procedures. It is possible, however, that mechanical properties of the tubes prevent the creation of certain tube sets with specific desired properties, (eg, very small radius of curvature). In these cases, it would be necessary to reconsider the robot design and potentially the access site to meet these constraints. Transjugular access was adopted as an initial entry route based on the procedure and to ensure high tip stiffness. The current TDP design can be easily adapted to a subclavian or transapical approach. Scaling up the length, while maintaining tip stiffness for transradial and transfemoral access, is a topic of future investigation.

When the PFO is sealed and the tissue approximation device is in its final configuration, the ratchet rail extends into the RA by a distance varying between 5 and 15 mm depending on the thickness of the approximated tissue. Although this protrusion is not sufficiently long to create tissue contact with the RA free wall, it is still exposed to the blood flow. The protruding length can be minimized by using devices with lengths matched to tissue thickness or through a design modification enabling detachment of the protruding portion.

The animal experiments were performed in a swine model. Although the anatomy of the porcine heart very closely resembles that of the human heart, there are several differences.[16] In particular, the area of the true atrial septum is smaller in a swine and represented by the floor of the fossa ovale. This resulted in the creation of smaller PFO defects in comparison with most of the clinical situations in humans.

Conclusions

Beating-heart image-guided percutaneous PFO closure can be successfully achieved using a novel robotic TDP and metal MEMS tissue approximation device. This technology is being developed further and could serve as a platform for reconstructive intracardiac procedures that are currently performed through open surgery.

Sources of Funding

This work was supported by National Institutes of Health National Heart, Lung, and Blood Institute Award No. R01HL087797 (Dr Dupont).

Disclosures

Dr Folk and A.L. Cohen were, and R. Chen is, employed by Microfabrica Inc, manufacturers of the tissue approximation device.

References

1. Généreux P, Head SJ, Van Mieghem NM, Kodali S, Kirtane AJ, Xu K, Smith C, Serruys PW, Kappetein AP, Leon MB. Clinical outcomes after

transcatheter aortic valve replacement using valve academic research consortium definitions: a weighted meta-analysis of 3,519 patients from 16 studies. *J Am Coll Cardiol*. 2012;59:2317–2326.
2. Chiam PT, Ruiz CE. Percutaneous transcatheter mitral valve repair: a classification of the technology. *J Am Coll Cardiol Cardiovasc Interv*. 2011;4:1–13.
3. Calvert PA, Rana BS, Kydd AC, Shapiro LM. Patent foramen ovale: anatomy, outcomes, and closure. *Nat Rev Cardiol*. 2011;8:148–160.
4. Carroll JD, Saver JL, Thaler DE, Smalling RW, Berry S, MacDonald LA, Marks DS, Tirschwell DL; for the Respect Investigators. RESPECT Clinical Trial – the final results with primary end point analyses. http://www.sjm.com/~/media/LandingPage/RESPECT/TCT%20RESPECT%2010–25%20Final.ashx. Accessed December 12, 2012.
5. Carrozza JP Jr. Robotic-assisted percutaneous coronary intervention–filling an unmet need. *J Cardiovasc Transl Res*. 2012;5:62–66.
6. Pappone C, Vicedomini G, Manguso F, Gugliotta F, Mazzone P, Gulletta S, Sora N, Sala S, Marzi A, Augello G, Livolsi L, Santagostino A, Santinelli V. Robotic magnetic navigation for atrial fibrillation ablation. *J Am Coll Cardiol*. 2006;47:1390–1400.
7. Gang ES, Nguyen BL, Shachar Y, Farkas L, Farkas L, Marx B, Johnson D, Fishbein MC, Gaudio C, Kim SJ. Dynamically shaped magnetic fields: initial animal validation of a new remote electrophysiology catheter guidance and control system. *Circ Arrhythm Electrophysiol*. 2011;4:770–777.
8. Yokoyama K, Nakagawa H, Shah DC, Lambert H, Leo G, Aeby N, Ikeda A, Pitha JV, Sharma T, Lazzara R, Jackman WM. Novel contact force sensor incorporated in irrigated radiofrequency ablation catheter predicts lesion size and incidence of steam pop and thrombus. *Circ Arrhythm Electrophysiol*. 2008;1:354–362.
9. Dupont PE, Lock J, Itkowitz B, Butler E. Design and control of concentric-tube robots. *IEEE Trans Robot*. 2010;26:209–225.
10. Butler E, Folk C, Cohen A, Vasilyev NV, Chen R, del Nido PJ, Dupont PE. Metal MEMS tools for beating-heart tissue approximation. *IEEE Int Conf Robot Autom*. 2011:411–416.
11. Cohen A, Zhang G, Tseng F-G, Frodis U, Mansfeld F, Will P. EFAB: rapid, low-cost desktop micromachining of high aspect ratio true 3-D MEMS. *Conf Proc IEEE Int Conf MEMS*. 1999:244–251.
12. Gosline AH, Vasilyev NV, Butler EJ, Folk C, Cohen A, Chen R, Lang N, Del Nido PJ, Dupont PE. Percutaneous intracardiac beating-heart surgery using metal MEMS tissue approximation tools. *Int J Rob Res*. 2012;31:1081–1093.
13. Vasilyev NV, Kawata M, DiBiasio CM, Durand KV, Hopkins J, Traina ZJ, Slocum AH, del Nido PJ. A novel cardioport for beating-heart, image-guided intracardiac surgery. *J Thorac Cardiovasc Surg*. 2011;142:1545–1551.
14. Mahvash M, Dupont P. Stiffness control of surgical continuum manipulators. *IEEE Trans Robot*. 2011;27:334–345.
15. Kutty S, Sengupta PP, Khandheria BK. Patent foramen ovale: the known and the to be known. *J Am Coll Cardiol*. 2012;59:1665–1671.
16. Crick SJ, Sheppard MN, Ho SY, Gebstein L, Anderson RH. Anatomy of the pig heart: comparisons with normal human cardiac structure. *J Anat*. 1998;193(pt 1):105–119.